Synthetic Metals 213 (2016) 34–41

Contents lists available at ScienceDirect

Synthetic Metals

journal homepage: www.elsevier.com/locate/synmet

Electrospinning of doped and undoped-polyaniline/poly(vinylidene fluoride) blends

Claudia Merlini[a], Alessandro Pegoretti[b], Thiago Medeiros Araujo[b], Sílvia D.A.S. Ramoa[a], Wido H. Schreiner[c], Guilherme Mariz de Oliveira Barra[a,*]

[a] Mechanical Engineering Department, Federal University of Santa Catarina (UFSC), Florianópolis, SC, Brazil
[b] Department of Industrial Engineering, University of Trento, 38123 TN, Italy
[c] Physics Department, Federal University of Paraná, Curitiba (UFPR), PR, Brazil

ARTICLE INFO

Article history:
Received 21 November 2015
Accepted 28 December 2015
Available online xxx

Keywords:
Electrospinning
Polyaniline
Emeraldine base
Poly(vinylidene fluoride)

ABSTRACT

Electrospun mats have been prepared by blending emeraldine base (EB) or DBSA-doped polyaniline (PANI.DBSA) with poly(vinylidene fluoride) (PVDF). In order to understand the effect of doped and undoped PANI on the structure and properties of PVDF/PANI mats, the electrical conductivity, doping degree and morphology of the electrospun mats were investigated. The effect of PANI.DBSA and EB content on the properties of PVDF solution and fibers morphology was investigated. The addition of either doped or undoped PANI increases the viscosity of the PVDF solution, but the ionic conductivity was changed significantly by adding doped PANI. The PVDF/EB fibers manifested a core-sheath structure, while PANI agglomerates were homogeneously distributed in the PVDF/PANI.DBSA. This morphology associated to the high porosity of mat resulted in insulating mats, even when 23 wt% of PANI salt was used and high doping levels were achieved. The PVDF/EB mats obtained from electrospinning displayed a considerable doping level, indicating that the electrical field could induce the protonation of PANI.

1. Introduction

Electrospinning of intrinsically conducting polymers (ICP), such as polypyrrole (PPy), polyaniline (PANI) and poly(3,4-ethylene-dioxythiophene) (PEDOT) into non-woven mats provides the possibility to obtain fibrous structures with new features and improved properties when compared to bulk materials [1]. An advantage of electrospun mats based on intrinsically conducting polymer is the possibility to associate the electrical conductivity of ICP, with the three-dimensional fiber network of the electrospun mats [2]. These characteristics associated with the high surface area and very high porosity of mats, make these materials potentially interesting for a wide range of applications, as for example, pressure sensors [3], humidity sensors [4], devices for hydrogen storage [5], for biomedical applications such as tissue engineering [6], and others.

The intrinsically conducting polymers display inherently poor solubility in common solvents, which originates from strong interchain and intrachain interactions [7,8]. Due to their poor solubility, low molecular weights and rigid backbone structure, they cannot be easily electrospun [9]. In order to overcome the spinnability problem of conducting polymer, various routes are reported to obtain conductive fibers by electrospinning [2]. The most common routes described in the open scientific literature are: (i) coating of insulating mats by using conducting polymers [2,6,10,11]; (ii) electrospinning of blends comprising of insulating and conducting polymers [2,8,12–16]; and (iii) coaxial electrospinning [17,18]. Each of these methods has its advantages and limitations. The most widely used method to produce electrospun mats based on intrinsically conducting polymer is the second one (spinning of polymer blends). In fact, the use of a carrier-insulating polymer blend can improve the spinability of the ICPs and provides the resulting mat with the required mechanical and functional properties [3].

Among the conducting polymers, PANI is particularly interesting for producing electrospun mats due its easy synthesis, high environmental stability and high electrical conductivity. Moreover, PANI can exist in a variety of forms with various degrees of protonation, varying from fully reduced leucoemeraldine (LE) to half oxidized emeraldine base (EB) and to fully oxidized pernigraniline (PE) [19]. The emeraldine base (EB) is normally doped by protonic acids in order to obtain a conducting form of

* Corresponding author at: Mechanical Engineering Department, UFSC, Campus Universitário Trindade, Caixa Postal 476, 88040-900 Florianópolis/SC, Brazil.
E-mail addresses: claudia.merlini@ufsc.br (C. Merlini), g.barra@ufsc.br (G.M.d.O. Barra).

http://dx.doi.org/10.1016/j.synthmet.2015.12.024
0379-6779/

polyaniline, i.e., emeraldine salt (ES) [20], and then blended with insulating polymers to be electrospun. Works in the literature have reported the electrospinning of blends composed of poly-(ethylene oxide) (PEO)/PANI and poly(methyl methacrylate) (PMMA)/PANI [14]; polystyrene (PS)/PANI, PMMA/PANI, PEO/PANI and polycarbonate (PC)/PANI [15]; PEO/PANI [21,22]; poly(vinyl butyral) (PVB)/PANI [4]; poly(3-hydroxybutyric acid) (PHB)/PANI [23]; nylon-6 (PA6)/PANI [24], poly(L-lactic acid) (PLA)/PANI [25], among others.

A wide range of electrical conductivity values have been reported in the literature for electrospun mats based on PANI, with electrical behavior ranging from insulating to conducting. These differences have been attributed to the intrinsic conductivities of insulating polymer and ICP, compatibility of both materials, conducting polymer content, type of dopant and the final morphology of the fibers. For example, conductivities as high as 8.1 S cm^{-1} and 2.3 × 10^{-2} S cm^{-1} have been reported by Zhang and Rutledge [14], for PEO/PANI and PMMA/PANI electrospun mats containing 67 wt% and 25 wt% of PANI, respectively. However, the authors reported that the electrical conductivities of the PEO/PANI mats are higher than those of PMMA/PANI mats for the same weight fraction of PANI, due to the difference on the intrinsic conductivities of PEO (∼10^{-6} S cm^{-1}) and PMMA (∼10^{-10} S cm^{-1}). On the other hand, some authors have been reported an insulating behavior for electrospun mats based on conducting polymers. Wei, Lee, Kang and Mead [15] reported that electrospun mats of PS/PANI, PMMA/PANI, PC/PANI, and PEO/PANI displayed electrical conductivity lower than 10^{-13} S cm^{-1}. The authors attributed the insulating behavior to the inability to form conducting pathways due to the formation of isolated PANI agglomerates in the PMMA/PANI and PEO/PANI fibers. In the case of PS/PANI and PC/PANI mats, this behavior was attributed to the encasement of the PANI in the insulating polymer, as well as the porosity of the electrospun mats. Additionally, some works have reported the electrical conductivity for single fibers and in some cases, the nonwoven mats are compressed [12] or the insulating polymer is extracted [13] before the measurement.

The use of PANI salt in the solution increases the charge density and may affect the properties of the solution, especially the ionic conductivity, which can enhances the jet instability and can become difficult to prepare the electrospun mats [11,26]. However, to the best of our knowledge, there are no studies published in the open scientific literature concerning the development of electrospun mats based on insulating polymer and the EB. Based in this context, the aim of this study is to understand the effect of both PANI salt and base on the properties of solution and on the structure and electrical properties of electrospun mats. The electrospun mats of undoped and doped PANI blended with poly(vinylidene fuoride) (PVDF) were developed through direct electrospinning. The (PVDF) was selected for its unique pyroelectric/piezoelectric features.

2. Experimental

2.1. Materials

Polyaniline, emeraldine base (EB—molecular weight M_w ∼10,000), dodecylbenzenesulfonic acid (DBSA - 70 wt% solution in 2-propanol) and poly(vinylidene fluoride) (PVDF) (M_w of 534,000 g mol^{-1}) was purchased from Sigma–Aldrich. Dymethylformamide (DMF) (99.8%) and acetone (99.5%) were purchased

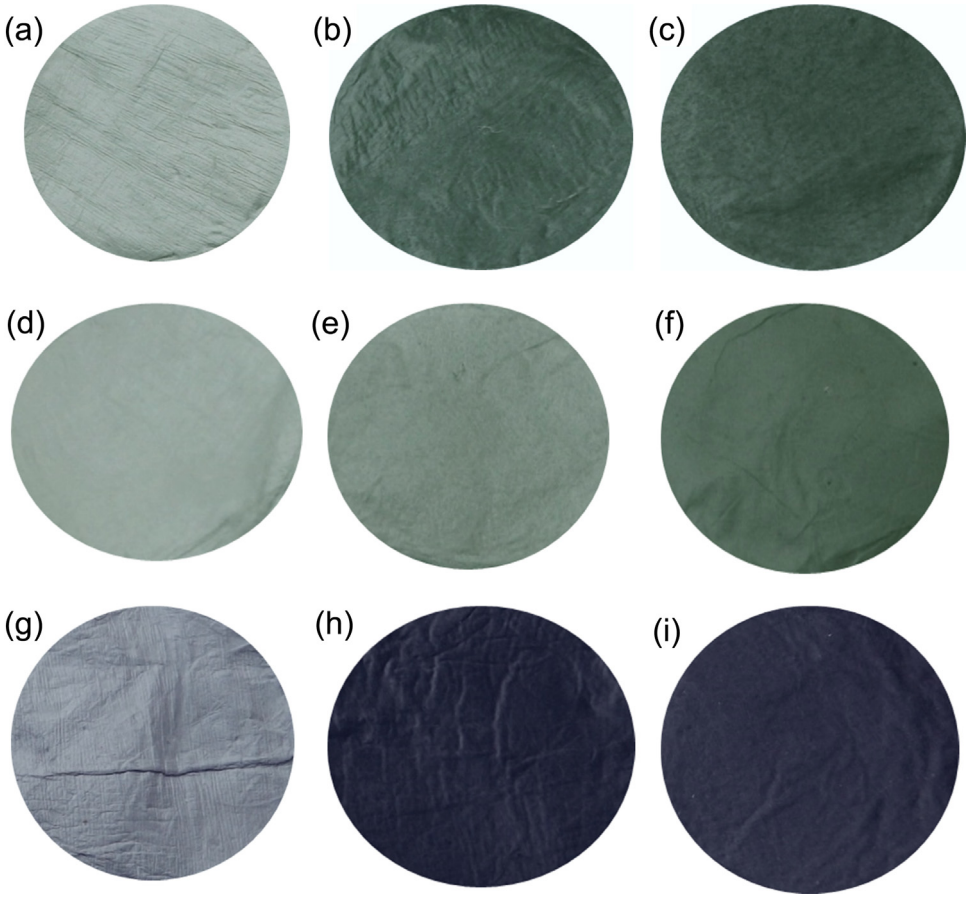

Fig. 1. Photographs of electrospun mats: (a) PVDF/EB_3, (b) PVDF/EB_13, (c) PVDF/EB_23, (d) PVDF/PANI.DBSA_3, (e) PVDF/PANI.DBSA_13 and (f) PVDF/PANI.DBSA_23. The photographs of PVDF/EB mats after treatment with alkaline solution is also reported (g–i).

Table 1
Electrical resistivity and measured content of PANI in the PVDF/PANI electrospun mats.

Sample	Electrical resistivity (Ω cm)	Measured PANI content in the blend (wt%)[a]	Nominal PANI content in starting solutions (wt%)
PVDF	$(2.7 \pm 1.4) \times 10^{15}$	0	0
PVDF/EB_3	$(6.4 \pm 1.2) \times 10^{14}$	1.70	3
PVDF/EB_13	$(2.0 \pm 1.3) \times 10^{14}$	11.13	13
PVDF/EB_23	$(5.1 \pm 0.9) \times 10^{12}$	17.70	23
PVDF/PANI.DBSA_3	$(7.1 \pm 1.3) \times 10^{13}$	1.3	3
PVDF/PANI.DBSA_13	$(8.9 \pm 1.6) \times 10^{13}$	8.7	13
PVDF/PANI.DBSA_23	$(1.5 \pm 1.0) \times 10^{12}$	14.15	23

[a] Calculated from CHN analysis.

from Sigma–Aldrich and Merck, respectively. All materials were used without further purification.

2.2. Polyaniline doping

Doping of EB into PANI salt was performed using DBSA. First, 16.05 g of DBSA were dissolved in 50 mL of water and then EB was added. The mixture was then stirred for 24 h at 25 °C, precipitated in acetone, filtered and washed with acetone. Then, the EB was mixed with DBSA (EB/DBSA = 1/3 by molar ratio) and grinded in an agate mortar. In order to remove the excess of DBSA, the resulting DBSA-doped polyaniline (PANI.DBSA) was washed with acetone and dried under vacuum at room temperature.

2.3. Preparation of PVDF/PANI mats by electrospinning

PVDF was dissolved in DMF under stirring for 2 h at 70 °C resulting in a 20 wt% solution. After cooling, acetone was added to the solution under stirring in a DMF/acetone proportion of 75/25 by weight, according to Merlini, Barra, Medeiros Araujo and Pegoretti [3]. EB particles were inserted into the PVDF solution at various weight concentrations (up to 23 wt%). The suspensions were mechanically stirred for 10 min, and sonicated with an ultrasonic probe (Ultrasonic Processor UP400 S Hielscher, 50 W and 60 Hz), for 5 min. The suspensions were spun through a 5 mL syringe (needle with an internal diameter of 0.66 mm) coupled with a syringe pump (Harvard Apparatus 11 Plus) at a flow rate of 1.0 mL h^{-1}. An electric field was generated using a high voltage supply (Spellman SL30), which generates DC fields up to 30 kV. The positive pole was connected to the syringe needle and the collector plate was grounded. PVDF/PANI fiber mats were obtained using an applied voltage from 15 to 25 kV and needle-to-collector distance of 30 cm. The entire electrospinning process was performed at 25 °C and humidity of 60% and the fibers were collected on an aluminum foil. For comparison, PVDF containing PANI.DBSA was also electrospun using similar methodology. The samples have been denoted as PVDF/EB_*x* or PVDF/PANI.DBSA_*x*, where *x* represents the weight content of EB and PANI.DBSA, respectively, in the blend.

Table 2
Elemental analysis obtained by XPS technique of EB, PVDF and PVDF/PANI electrospun mats.

Sample	Area Ratio (Atom%)				
	C	N	O	S	F
EB	79.42	9.56	11.02	–	–
PVDF	18.01	–	–	–	81.99
PVDF/EB_13	48.50	1.15	1.20	–	49.15
PVDF/EB_23	49.09	1.00	2.89	–	47.02
PVDF/PANI.DBSA_23	56.97	1.07	3.96	0.9	38.81

2.4. Characterization techniques

The electrical conductivity of the PANI samples were measured using the four-probe standard method with a Keithley 6220 current source to apply the current and a Keithley Model 6517A electrometer to measure the potential difference, according to ASTM F42-93. The PANI samples were compacted using a hydraulic press, at pressures up to 3 MPa, into cylindrical forms with 25 mm in diameter. For high-resistivity electrospun mats, the measurements were performed using a Keithley 6517A electrometer connected to a Keithley 8009 test fixture, according to ASTM D-257 methodology, on circular specimens of 90 mm of diameter. Measurements of each sample were taken at least eight times at room temperature.

X-ray photoelectron spectrometry (XPS) measurements were obtained using an ESCA3000 VG spectrometer with an MgK-α X-ray source (1253.6 eV) operating at 150 W. The electron analyzer was operated in an ultra-high vacuum chamber, at 10^{-9} mBar. All binding energies were referenced to the C-1s neutral carbon peak (284.6 eV) in order to compensate the surface charging effects.

Scanning electron microscopy (SEM) images were obtained using a Jeol model JSM-6390LV microscope. The samples were coated with gold and analyzed under an accelerating vontage of 10 or 15 kV.

The viscosity of the solutions was evaluated using a viscometer model ViscoTester 6 L Thermo Haake using the L4 spindle and 12 rpm at 25 °C.

The ionic conductivity of the solution was measured using a Bante Instrumental 950 equipment at 25 °C.

Transmission electron microscopy (TEM) was performed using a JEM-1011 microscope. The fibers were electrospun directly on the copper grid and analyzed using an acceleration voltage of 100 kV.

Elemental analysis (carbon, hydrogen and nitrogen) was carried out using a PerkinElmer CHN 2400 analyzer. The combustion process was held at 925 °C using pure oxygen (99.995%).

3. Results and discussion

PVDF/PANI fiber mats were prepared through electrospinning from PVDF solutions containing various fractions of emeraldine base (EB) and PANI salt (PANI.DBSA). Surprisingly, the electrospun mats from blends containing PVDF and EB (blue color) displayed a grayish green color, typical of PANI salt, according with the photographs showed in Fig. 1(a–c). The color of PVDF/EB mats is very close to the color of the mats prepared through electrospinning from PVDF solutions containing PANI.DBSA (Fig. 1d–f). This behavior indicates that the electrospinning could provide enough energy to protonate EB. When the electrospun PVDF/EB mats were treated with alkaline solution of ammonium hydroxide 0.1 M (Fig. 1g–i), their color changed from grayish green to grayish blue, indicating that the acid-base transition may have occurred.

Neat EB displays an electrical resistivity of $(1.7 \pm 0.3) \times 10^8$ Ω cm, while after doping with DBSA, and the occurrence

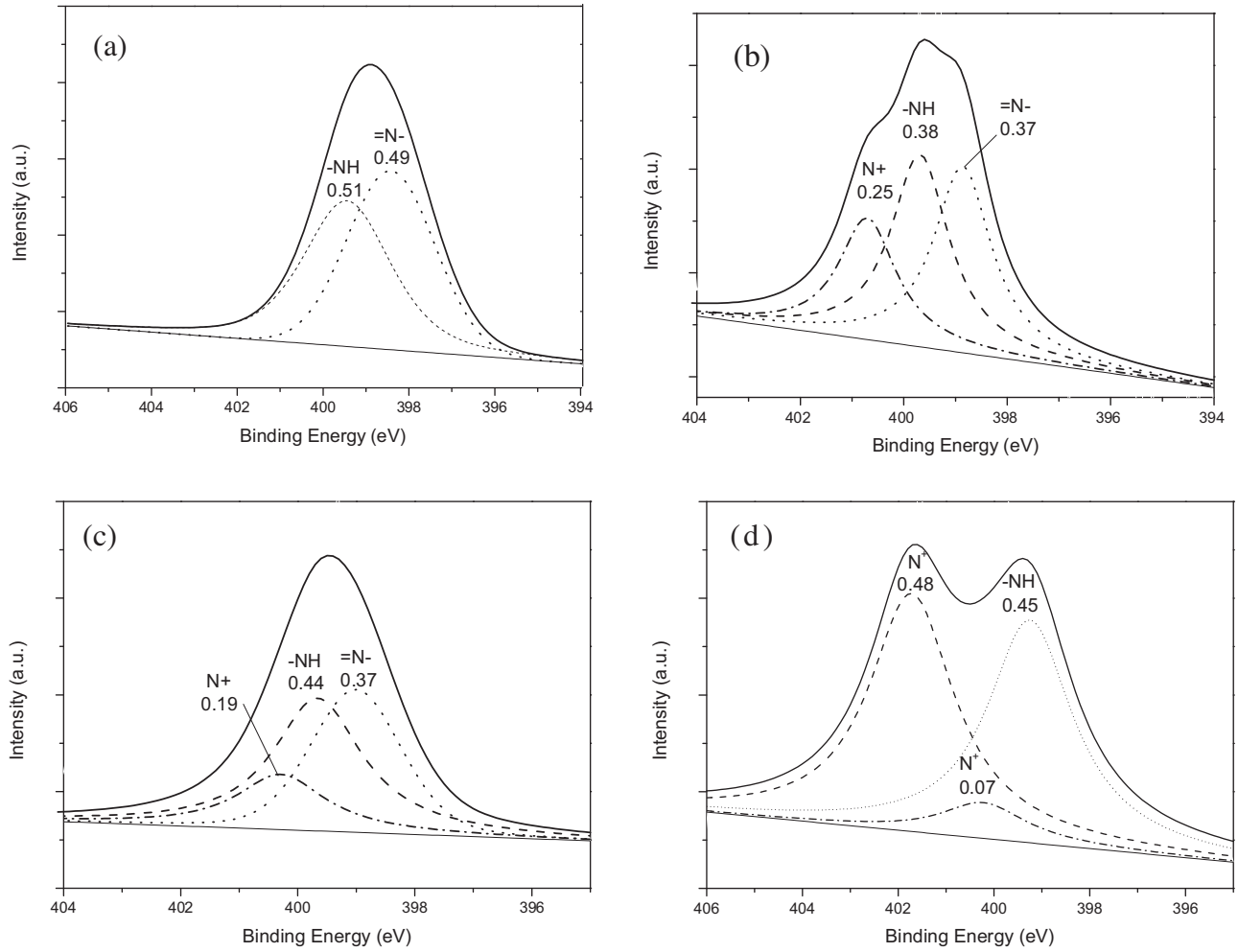

Fig. 2. XPS N 1s core level spectra of (a) EB and electrospun mats: (b) PVDF/EB_13, (c) PVDF/EB_23 and (d) PVDF/PANI.DBSA_23.

of the base-acid transition the electrical resistivity decreased to $0.33 \pm 0.2\,\Omega$ cm. The electrical conductivity measurements for electrospun PVDF and PVDF/PANI mats are reported in Table 1. PVDF/EB mats electrospun from solution containing undoped PANI showed electrical resistivity higher than $10^{12}\,\Omega$ cm, which are similar to PVDF/PANI.DBSA. This insulating behavior, for both PVDF/EB and PVDF/PANI.DBSA mats, indicates that the electrical percolation threshold is not reached even for PANI.DBSA loading of 23 wt%. Nevertheless, it is important to point out that blends containing more than 23 wt% of PANI are not suitable for the electrospinning technique due to their high viscosity. The second issue that needs to be highlighted is that the technique used in this work to measure the electrical resistivity provides volume resistivity, which does not take into account the electrospun mat porosity. Therefore, the electrical resistivity measured for the electrospun mats are apparent resistivity and do not apply to single fibers which should display a little lower electrical resistivity [16]. The electrical conductivity measured for mats in the present work is comparable to those reported for different electrospun mats such as: PS/PANI, PMMA/PANI, PC/PANI and PEO/PANI [15]; PVDF/PPy [2]; PLA/PANI [27] and polyvinylpyrrolidone (PVP)/PEDOT [28]. It is important to note that in all the above cited works the doped form of conducting polymers were used in solution.

Table 3
The proportion of N species and doping degree of pure PANI and electrospun mats obtained by XPS technique.

Samples	Proportion of			Doping Level
	=N—	—NH—	N^+	(%)
EB	0.49	0.51	–	–
PVDF/EB_13	0.37	0.38	0.25	25
PVDF/EB_23	0.37	0.44	0.19	19
PVDF/PANI.DBSA_23	–	0.45	0.55	55

The PANI content in each electrospun mat (Table 1) was calculated from the different nitrogen content of the blend and neat PANI [3]. As expected, the PANI amount on the PVDF/PANI electrospun mats increases significantly with increasing polyaniline concentration in the starting solution. However, for all compositions the amount of PANI in the electrospun mats estimated by elemental analysis is slightly lower than the amount of PANI in the starting solutions. This indicates that PANI could not be dispersed homogeneously in the suspension and consequently it could be only partially transfered in the electrospun mats.

XPS analysis was used to estimate the doping level of the PVDF/PANI samples and investigate the possibility of EB protonation during electrospinning, once the electrical conductivity was similar for both PVDF/EB and PVDF/PANI.DBSA mats. From this technique, the elements involved can be identified from the characteristic binding energy (BE) and the peak intensity can be directly associated to the atomic concentration on the sample surface [29]. Additionally, from the N1s core-level spectrum, the

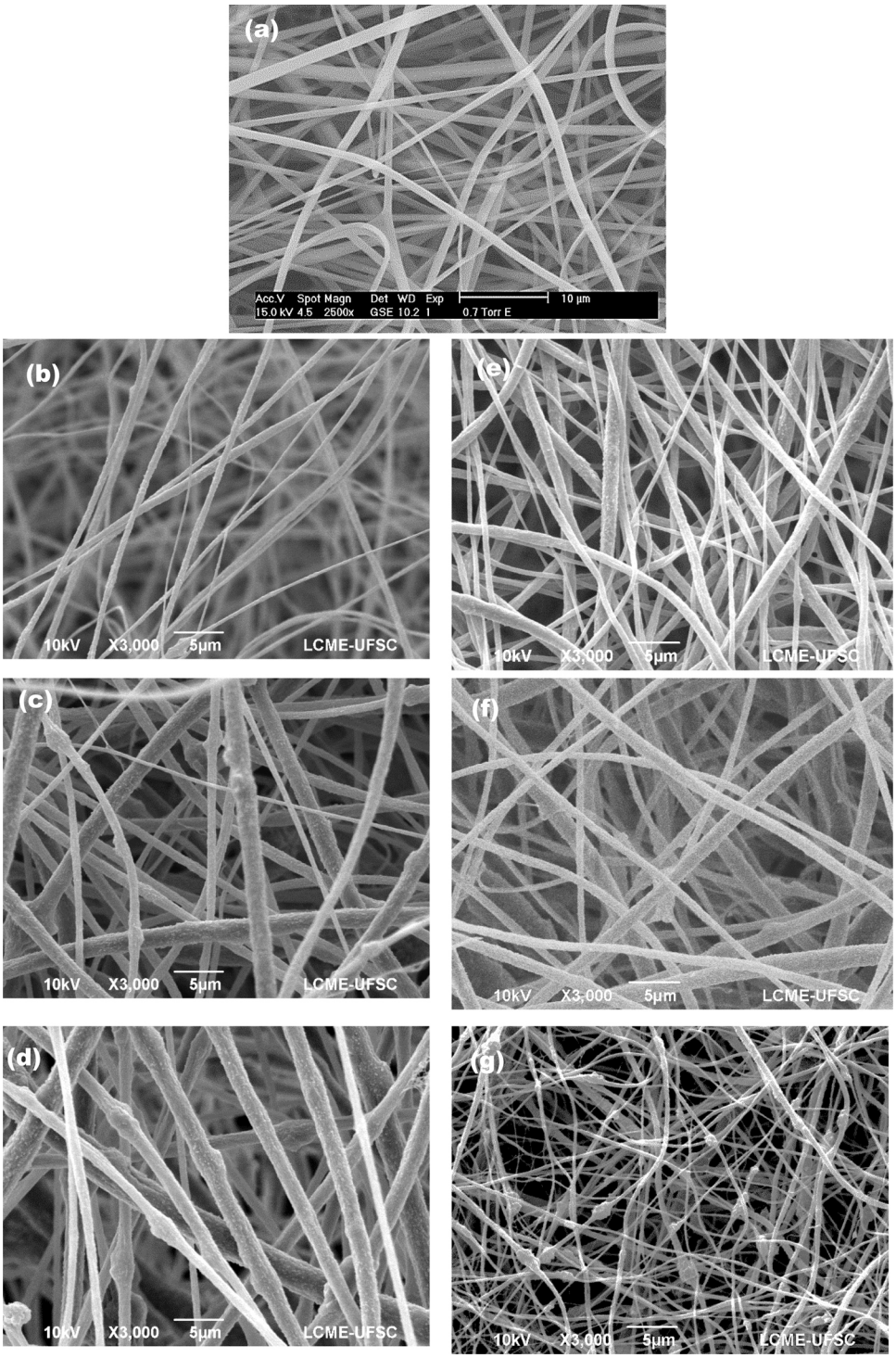

Fig. 3. SEM micrographs of electrospun mats of (a) neat PVDF, (b) PVDF/EB_3, (c) PVDF/EB_13 (d) PVDF/EB_23, (e) PVDF/PANI.DBSA_3, (f) PVDF/PANI.DBSA_13 (g) PVDF/PANI.DBSA_23.

various intrinsic redox states of PANI and the different neutral and positive nitrogen species corresponding to a protonation level can be identified and quantified [30,31].

Table 2 presents the surface composition obtained from XPS survey scan of PVDF, PANI and PVDF/EB and PVDF/PANI.DBSA mats. EB shows the presence of carbon (C 1s −283.0 eV), nitrogen (N 1s −399.3 eV) as well as oxygen (O 1s −530.4 eV). The elements carbon and nitrogen are originated from PANI backbone and the oxygen can be originated from surface partial oxidation [10,32]. The XPS survey scan of PVDF shows the presence of fluorine (F 1s) at 691.2 eV and carbon (C 1s) at 289.4 and 293.9 eV assigned to CH_2 e CF_2, respectively [33]. As reported by Barra, Leyva, Gorelova, Soares and Sens [34], PANI.DBSA prepared by the same methodology, also present sulfur (S) due to the presence of DBSA. PVDF/EB and PVDF/PANI.DBSA electrospun mats display carbon, nitrogen, oxygen, fluorine and sulfur atoms from both PANI and PVDF.

Fig. 2 shows the deconvoluted N 1s core level spectra of EB, PVDF/EB and PVDF/PANI.DBSA electrospun mats. The N 1s

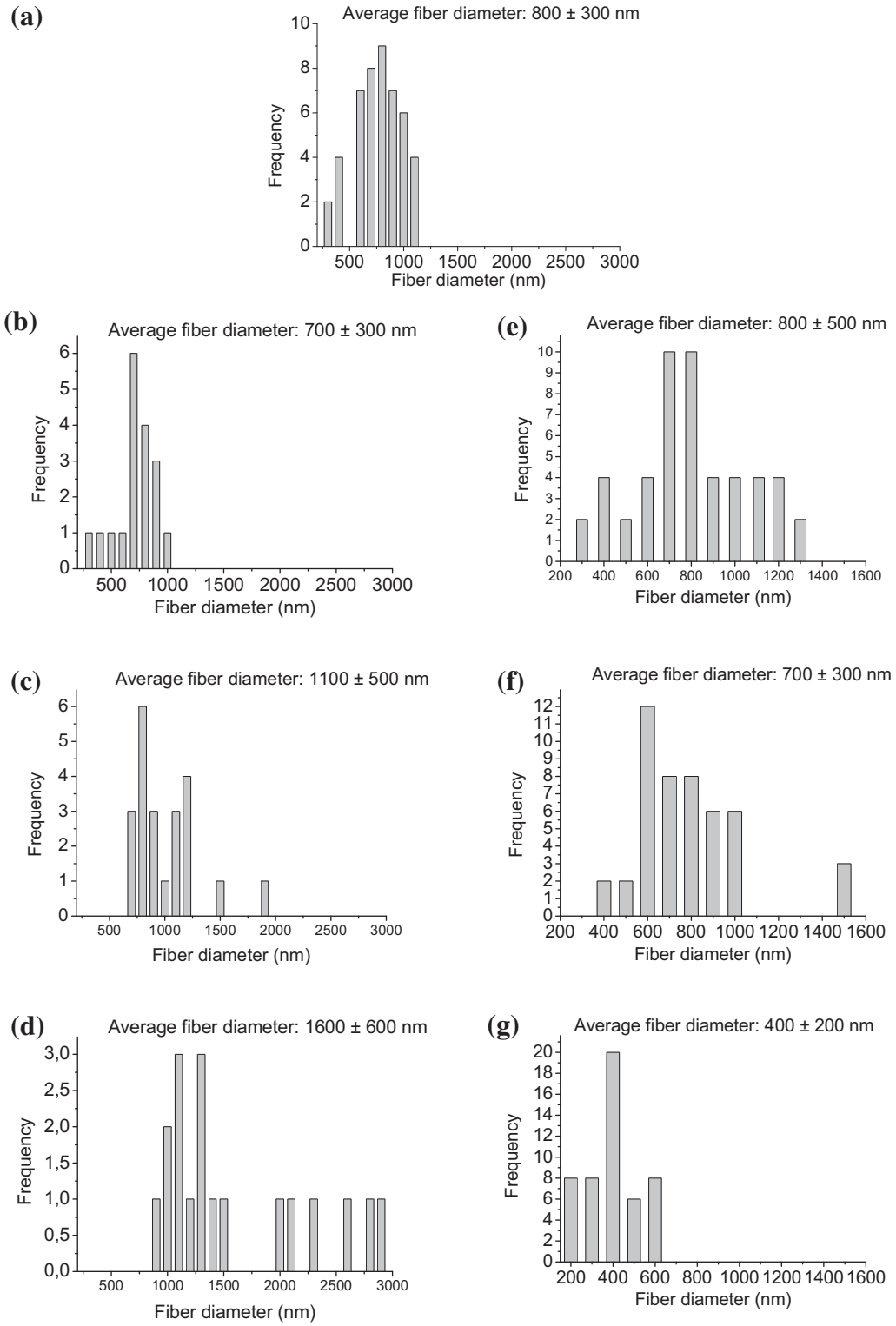

Fig. 4. Histograms of the fiber diameters and the average fiber diameter of electrospun mats of (a) neat PVDF, (b) PVDF/EB_3, (c) PVDF/EB_13 (d) PVDF/EB_23, (e) PVDF/PANI. DBSA_3, (f) PVDF/PANI.DBSA_13 (g) PVDF/PANI.DBSA_23.

spectrum of EB can be deconvoluted into two peaks, associated to the major components, centered at 398.4 and 399.5 eV, assigned to the imine and amine, respectively [35]. The N 1s deconvoluted results of EB show that the imine to amine ratio is almost 1:1 (Table 3), similar to the theoretical values, indicating emeraldine base structure [29,35]. The N 1s core-level spectra of PVDF/EB electrospun mats from solution containing 13 and 23 wt% of EB, reveals the presence of an additional peak at around 400.5 eV attributed to the positively charged nitrogen [34]. The proportion of this peak was found to be 0.25 and 0.19 for mats electrospun from 13 and 23 wt% of EB (Table 3), which corresponds to the protonation degree [34]. This behavior indicates that electrospinning can be able to induce the protonation of PANI base when it is electrospun into mats. The ability to achieve certain doping level

Table 4
Ionic conductivity and apparent viscosity of solution, and voltage applied during electrospinning process.

Sample	Ionic Conductivity (μS)	Apparent viscosity (mPa s)	Voltage during electrospinning (kV)
PVDF	1.0 ± 0.3	610.0 ± 1.5	15
PVDF/EB_3	5.1 ± 0.2	683.3 ± 5.7	15
PVDF/EB_13	6.4 ± 0.2	910.0 ± 5.6	15
PVDF/EB_23	6.4 ± 0.2	1100.0 ± 3.7	15
PVDF/PANI.DBSA_3	120.8 ± 0.7	850.1 ± 5.1	16
PVDF/PANI.DBSA_13	979.0 ± 5.1	960.2 ± 7.4	22
PVDF/PANI.DBSA_23	1219.8 ± 4.7	1130.1 ± 7.6	25

of PANI by electrospinning can be tentatively explained by some interaction with the PVDF, which can release proton when it is exposed to electrical field. Another possible explanation could be attributed to fact that the solvent can act as a secondary dopant [36], which leads to doping of PANI base.

For PVDF/PANI.DBSA electrospun mat, all the imine groups have been protonated, since the peak at ~398.9 eV has completely disappeared. However, in this case, high doping level (55%) is not enough to provide electrical conductivity to the membrane, since the porosity of the electrospun mat and the isolated PANI agglomerates in the fibers do not allow the formation of conducting pathways. Lower doping levels of PVDF/EB electrospun mats (from 19 to 25 wt%) were obtained in the XPS studies when compared with PVDF/PANI.DBSA electrospun mat (55%). This behavior can be associated to the high doping level of PANI.DBSA (48% as reported by Barra, Leyva, Gorelova, Soares and Sens [34]) as compared with the undoped EB.

Fig. 3 illustrates SEM images of electrospun mats of neat PVDF, PVDF/EB and PVDF/PANI.DBSA. The electrospun mats are composed of three-dimensional random fibrous network. As shown in

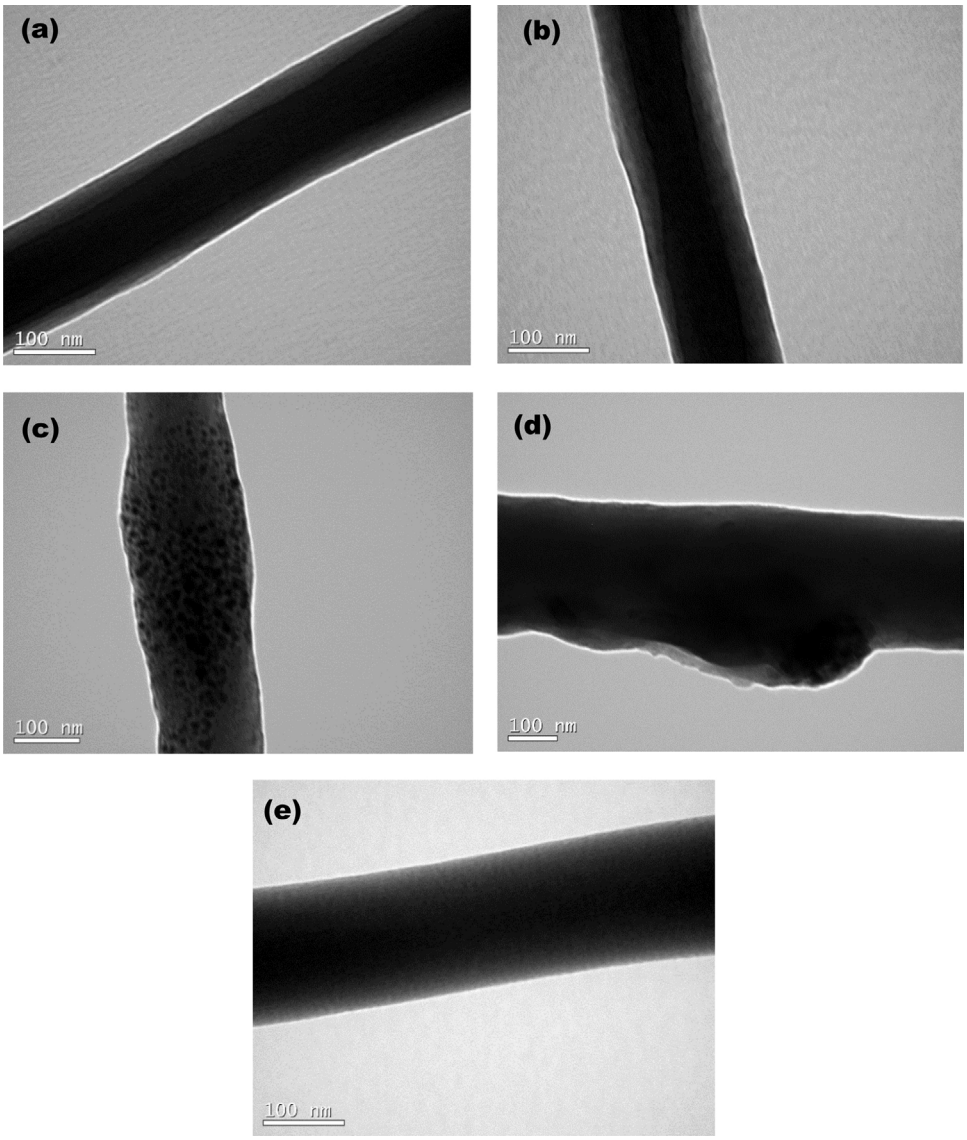

Fig. 5. TEM micrographs of electrospun mats of (a and b) PVDF/EB _13, (c and d) PVDF/PANI.DBSA_13 and (e) neat PVDF.

these micrographs, the morphology typically shows uniforms fibers, although, as the PANI content increases, aggregate bead structures can also be observed in some fibers, especially on mats containing 23 wt% of PANI.

The average diameter of PVDF/EB fibers, measured from SEM micrographs, increases substantially with increasing EB content, as shown in Fig. 4. This behavior can be attributed to the solution viscosity increases (Table 4), which makes difficult the ejection of the polymer solution from the needle [37]. The ionic conductivities of PVDF/EB solutions are quite similar to neat PVDF, thereby it is not possible to correlate ionic conductivity directly to the fiber diameter.

For the PVDF/PANI.DBSA solution, with increasing the PANI.DBSA content both viscosity and ionic conductivity of system increased substantially. As a result, the process becomes more difficult to be controlled. In order to avoid electrospraying of PVDF/PANI.DBSA solution, the voltage applied during the electrospinning process was adjusted from 15 to 25 kV (Table 4). One of the effects of increasing the voltage is the reduction of the fiber diameter [3], as observed in Fig. 4. Additionally, the increase of conductivity of the solution may increase the charge density and higher elongation forces are imposed to the jet, which enhances the whipping instability, leading to thinner fiber diameters [26].

The microstructure of electrospun fibers containing 13 wt% of EB or PANI.DBSA and neat PVDF was observed by TEM, as showed in Fig. 5. PVDF/EB fibers (Fig. 5a and b) present core sheath structures with the EB polymer phase encased by the insulating polymer (PVDF). Thus, the encasement of the EB in the PVDF, as well as the porosity of the electrospun mat could explain the observed insulating behavior [15]. In contrast, PVDF/PANI.DBSA fibers display a morphology different from PVDF/EB fibers. As shown in Fig. 5c and d, these fibers did not form uniform core-sheath structures, but are comprised of PANI.DBSA agglomerates along the fiber. The PANI agglomerates are discontinuous and dispersed, in contrast to the core-sheath structures of PVDF/EB fibers. One possible explanation could be attributed to the high-surface tension of PANI.DBSA, which greatly increases the surface tension of the entire solution, thus increasing the aggregation tendency of PANI [15]. This morphology does not provide a conductive pathway or charge-carrier mobility along the fiber axis and consequently, electrospun fibers display high electrical resistivity.

4. Conclusions

Non-woven mats were obtained through electrospinning of PVDF/EB and PVDF/PANI.DBSA blends. Comparing the systems it can be noted that both salt or base PANI affect the solution properties and have an influence on the process, morphology and the fibers diameter. The electrospinning of solution with PANI base is easy to be performed when compared with solution containing PANI salt, since both viscosity and ionic conductivity of solution are greatly modified by the addition of doped PANI. Consequently, in order to obtain uniforms fibers, the voltage applied to neat PVDF need to be adjusted when PANI salt is used, which result in thinner fibers. The electrospun mats from solution containing EB displayed a grayish green color, typical of PANI salt, similar to the color of PVDF/PANI.DBSA mats. In fact, the doping level of PVDF/EB obtained from XPS analysis was in the range from 19 to 25%, indicating that the electrospinning could be able to induce some protonation on the PANI. The possibility to protonate polyaniline through a free-acid process can be interesting for a wide range of applications. The PVDF/EB mats behave as an insulating material due to its porosity and the structure, like core-sheath, which result in high values of electrical resistivity. This same insulating behavior was observed to PVDF/PANI.DBSA mats due to the inability to form continuous pathways through the fibers. For PVDF/PANI.DBSA a doping level higher than 50% was not enough to reach electrical conductivity similar to that of neat PANI. The results reported in this study showed that the introduction of doped and undoped PANI into fibers mats by mixing with PVDF does not provide a good level of electrical conductivity.

Acknowledgements

The authors gratefully acknowledge the financial support of the Conselho Nacional de Desenvolvimento Científico e Tecnológico—CNPq through the program “Science Without Borders”, Coordenação de Aperfeiçoamento de Pessoal de Ensino Superior—CAPES, and Fundação de Amparo à Pesquisa e Inovação do Estado de Santa Catarina—FAPESC. We are also very grateful to Central Electronic Microscopy Laboratory, (LCME-UFSC) for the microscopy analysis.

References

[1] X. Li, X. Hao, H. Yu, H. Na, Mater. Lett. 62 (2008) 1155–1158.
[2] C. Merlini, G.M.D.O. Barra, S.D.A.D.S. Ramoa, G. Contri, R.S. d. Almeida, M.A. D'Ávila, B.G. Soares, Frontiers in Materials 2 (2015) 1–6.
[3] C. Merlini, G.M.O. Barra, T. Medeiros Araujo, A. Pegoretti, RSC Adv. 4 (2014) 15749–15758.
[4] Q. Lin, Y. Li, M. Yang, Sens. Actuators B: Chem. 161 (2012) 967–972.
[5] S.S. Srinivasan, R. Ratnadurai, M.U. Niemann, A.R. Phani, D.Y. Goswami, E.K. Stefanakos, Int. J. Hydrogen Energy 35 (2010) 225–230.
[6] J.Y. Lee, C.A. Bashur, A.S. Goldstein, C.E. Schmidt, Biomaterials 30 (2009) 4325–4335.
[7] M. Yanilmaz, F. Kalaoglu, H. Karakas, A.S. Sarac, J. Appl. Polym. Sci. 125 (2012) 4100–4108.
[8] I.S. Chronakis, S. Grapenson, A. Jakob, Polymer 47 (2006) 1597–1603.
[9] M. Yanılmaz, A.S. Sarac, Text. Res. J. 84 (2014) 1325–1342.
[10] C. Merlini, R.d.S. Almeida, M.A. D'Ávila, W.H. Schreiner, G.M.d.O. Barra, Mater. Sci. Eng.: B 179 (2014) 52–59.
[11] H. Park, S.J. Lee, S. Kim, H.W. Ryu, S.H. Lee, H.H. Choi, I.W. Cheong, J.-H. Kim, Polymer 54 (2013) 4155–4160.
[12] T.S. Kang, S.W. Lee, J. Joo, J.Y. Lee, Synth. Met. 153 (2005) 61–64.
[13] K. Sujith, A.M. Asha, P. Anjali, N. Sivakumar, K.R.V. Subramanian, S.V. Nair, A. Balakrishnan, Mater. Lett. 67 (2012) 376–378.
[14] Y. Zhang, G.C. Rutledge, Macromolecules 45 (2012) 4238–4246.
[15] M. Wei, J. Lee, B. Kang, J. Mead, Macromol. Rapid Commun. 26 (2005) 1127–1132.
[16] A. Laforgue, L. Robitaille, Synth. Met. 158 (2008) 577–584.
[17] H. Dong, V. Nyame, A.G. MacDiarmid, W.E. Jones, J. Polym. Sci. B: Polym. Phys. 42 (2004) 3934–3942.
[18] A. Sarvi, V. Chimello, A.B. d. Silva, R.E.S. Bretas, U. Sundararaj, Plast.Res. Online (2014) 1–3.
[19] D. Chen, Y.-E. Miao, T. Liu, ACS Appl. Mater. Interfaces 5 (2013) 1206–1212.
[20] Y. Xia, J.M. Wiesinger, A.G. MacDiarmid, A.J. Epstein, Chem. Mater. 7 (1995) 443–445.
[21] I.D. Norris, M.M. Shaker, F.K. Ko, A.G. MacDiarmid, Synth. Met. 114 (2000) 109–114.
[22] Y.-W. Lin, T.-M. Wu, J. Appl. Polym. Sci. 126 (2012) E123–E129.
[23] R. Fryczkowski, T. Kowalczyk, Synth. Met. 159 (2009) 2266–2268.
[24] H. Bagheri, A. Aghakhani, Anal. Chim. Acta 713 (2012) 63–69.
[25] P.H.S. Picciani, E.S. Medeiros, Z. Pan, W.J. Orts, L.H.C. Mattoso, B.G. Soares, J. Appl. Polym. Sci. 112 (2009) 744–753.
[26] P. Heikkila, A. Harlin, Exp. Polym. Lett. 3 (2009) 437–445.
[27] P.H.S. Picciani, E.S. Medeiros, Z. Pan, D.F. Wood, W.J. Orts, L.H.C. Mattoso, B.G. Soares, Macromol. Mater. Eng. 295 (2010) 618–627.
[28] J. Choi, J. Lee, J. Choi, D. Jung, S.E. Shim, Synth. Met. 160 (2010) 1415–1421.
[29] B. Sreedhar, M. Sairam, D.K. Chattopadhyay, P.P. Mitra, D.V.M. Rao, J. Appl. Polym. Sci. 101 (2006) 499–508.
[30] M.E. Leyva, G.M.O. Barra, M.M. Gorelova, B.G. Soares, M. Sens, J. Appl. Polym. Sci. 80 (2001) 626–633.
[31] E.T. Kang, K.G. Neoh, K.L. Tan, Prog. Polym. Sci. 23 (1998) 277–324.
[32] S. Golczak, A. Kanciurzewska, M. Fahlman, K. Langer, J.J. Langer, Solid State Ionics 179 (2008) 2234–2239.
[33] M.-Z. Li, J.-H. Li, X.-S. Shao, J. Miao, J.-B. Wang, Q.-Q. Zhang, X.-P. Xu, J. Membr. Sci. 405–406 (2012) 141–148.
[34] G.M.O. Barra, M.E. Leyva, M.M. Gorelova, B.G. Soares, M. Sens, J. Appl. Polym. Sci. 80 (2001) 556–565.
[35] K.L. Tan, B.T.G. Tan, E.T. Kang, K.G. Neoh, Phys. Rev. B 39 (1989) 8070–8073.
[36] S.J. Dahman, Polym. Eng. Sci. 39 (1999) 2181–2188.
[37] N. Bhardwaj, S.C. Kundu, Biotechnol. Adv. 28 (2010) 325–347.